Recibido: Abr. 2, 2025 | Aceptado: Jul. 21, 2024 | Publicado: Ago. 4, 2025

Simulation and technical analysis of an industrial-scale chitosan production process using computer-aided engineering

Simulación y análisis técnico del proceso de producción de quitosano a escala industrial mediante ingeniería asistida por computadora

DOI: https://doi.org/10.21803/ingecana.5.5.903

Eduardo Andres Aguilar Vasquez

Orcid: https://orcid.org/0000-0003-1744-1622

Ingeniero, Universidad de Cartagena, eaguilarv@unicartagena.edu.co

Samir Meramo-Hurtado

Orcid: https://orcid.org/0000-0002-9350-9898

 ${\tt Doctor, SMH\ Sustainability\ Consulting\ LLC, samhur@biosustain.dtu.dk}$

Ángel Darío González-Delgado Orcid: https://orcid.org/0000-0001-8100-8888

Doctor, Universidad de Cartagena, agonzalezd1@unicartagena.du.co

Abstract

This work aims to simulate and analyze a topology to produce chitosan from shrimp exoskeletons using computer-aided engineering. To achieve this, the commercial simulator Aspen Plus was used to replicate a block diagram based on representative data from the literature and experimental analyses. The simulation resulted in a process that produces 12,152 tons/year of chitosan from 57,000 tons/year of shrimp exoskeletons. Additionally, the simulation was validated by comparing the properties of the chitosan obtained with those reported in the literature. This validation yielded positive results, showing an accuracy above 88%, indicating that the assumptions made for the simulation were appropriate. Furthermore, the technical analysis showed that the process has a significant yield of 210.1 g per kilogram of raw material, along with a considerable technical efficiency of 63.4%. This value suggests that the process efficiently produces chitosan; however, there is still potential for improvement to increase its productivity.

Keywords: Bioprocess, Circular economy, Process engineering, Computer-aided, Chitosan.

Resumen

Este trabajo tiene como objetivo simular y analizar una topología para la producción de quitosano a partir de exoesqueletos de camarón mediante ingeniería asistida por computadora. Se utilizó el simulador comercial Aspen Plus para simular un proceso basado en datos representativos extraídos de la literatura y de análisis experimentales. La simulación produce 12.152 t/año de guitosano a partir de 57.000 t/año de exoesqueleto de camarón. La validación de la simulación al comparar con propiedades del quitosano reportadas en la literatura arrojó resultados positivos, con una exactitud superior al 88%, indicando que las consideraciones realizadas fueron adecuadas. Por otro lado, el análisis técnico mostró que el proceso tiene un rendimiento significativo de 210.1 g por kilogramo de materia prima, junto con una eficiencia técnica considerable del 63.4%. Este valor sugiere que el proceso produce quitosano de manera eficiente; sin embargo, aún existe un potencial de mejora para aumentar su productividad.

Palabras clave: Bioprocesos, Economía circular, Ingeniería de procesos asistida por computadora, Quitosano.

Cómo citar este artículo:

E. A. Aguilar Vasquez, S. M.-Hurtado y A. D. González-Delgado. «Simulation and technical analysis of an industrial-scale chitosan production process using computer-aided engineering». Ingente Americana, vol. 5, n°5, e-903, 2025. DOI: https://doi.org/10.21803/ingecana.5.5.903



⊕ ≥

Introduction

The adoption of the so-called 2030 Agenda for Sustainable Development and its 17 Sustainable Development Goals reinforced the need for a transition toward a green economy as a means to address climate change, biodiversity loss, water scarcity, and other challenges, while also tackling key social and economic issues [1]. This shift involves concepts such as the bioeconomy, which aims for a holistic transformation of the economy and society. This economy focuses on the industrial use of renewable biological resources as raw materials to produce energy, chemicals, and materials [2]. It also includes concepts of circular economy and clean production. In this context, biorefineries are being developed as technological vehicles that enable the valorization of various types of biomass through the development of innovative products via more sustainable production processes [3].

Seafood has become one of the most widely traded food products worldwide, reaching a global market value of USD 164.1 billion in 2018, and it is projected to reach USD 194 billion by 2027 [4]. This increase in consumption has led to a substantial rise in waste generation. Due to their composition, these residues have a relatively slow biodegradation rate, resulting in significant accumulation of processing waste. Inadequate disposal of this waste could have negative environmental impacts; therefore, alternatives for transforming this biomass into valuable products have received considerable attention in recent decades [5].

The reported chemical composition of crustacean exoskeletons consists of 20%-30% chitin, 30%-40% protein, and 30%-50% calcium phosphate/carbonate, which represents an attractive composition for chitosan extraction (the second most abundant biopolymer in nature) [6]. Chitosan is the partially deacetylated product of chitin (a natural aminopolysaccharide that serves as a structural material in crustaceans, insects, etc.) and is composed predominantly of β -(1>4)-2-amino-2-deoxy-D-glucose units (deacetylated units), and a smaller proportion (typically less than 20%) of β -(1>4)-2-acetamido-D-glucose (acetylated units) [7]. Thanks to this composition, chitosan has multidimensional application potential, including fields such as food and nutrition, pharmaceuticals, biotechnology, materials science, agriculture, and environmental protection, among others [8]. The conventional route for producing chitosan from shrimp shell waste involves the following processing steps: deproteinization (DP), demineralization (DM), depigmentation (DG), and alkaline deacetylation (AD) [9]. The chitin deacetylation step is particularly important, as the extent of this reaction determines the solubility of the product under acidic conditions [10].

In the case of Colombia, shrimp farming and

aquaculture production take place in areas along the Pacific Ocean, with an estimated flow of 2,400 tons per year, where nearly 20% of the shrimp's weight is discarded as waste. This waste generates environmental and public health problems, including the contamination of water sources, the attraction of vector-borne diseases, and the underutilization of residues with potential for producing value-added products [11]. Additionally, there is a lack of knowledge related to the optimal exploitation of this waste and the scaling-up of biomass conversion technologies, considering techno-economic, environmental, and social sustainability issues [12].

Since chitosan production technologies from chitin are still in the early stages of development (with low Technology Readiness Levels, TRL), many of these processes have only been reported at the laboratory scale [13]. In addition, there are challenges related to high production costs and the generation of wastewater effluents [14]. Therefore, it is important to develop models that enable the implementation of these technologies at an industrial scale, considering the specific characteristics and complexities of the processes involved. In this regard, the use of computational tools (grouped under the concept of Process Systems Engineering) becomes essential for the development and adoption of these technologies. These tools facilitate the design, operation, control, and optimization of processes [15]. Process simulation allows for the calculation of extended mass and energy balances, determination of separation yields, reaction rates, quantification of total process utility requirements, and estimation of physical-chemical properties of substances, among others [16]. This information serves as a foundation for evaluating the feasibility and performance of processes under sustainability criteria [17].

In the literature, there are studies that simulate, or model bioprocesses focused on the utilization of biomass derived from waste, by-products, and other sources. The extraction of chitin from crustacean shells was evaluated by using sustainability parame-

ters that considered techno-economic, environmental, and safety aspects [18]. The approach integrated the results through a hierarchical method to compare chemical and enzymatic processes for chitin extraction from this type of waste. On the other hand, the production of glycerol from corn oil was simulated using Aspen Hysys [19]. Posada et al. simulated and economically evaluated a process to produce poly(3-hydroxybutyric acid) (PHB) from crude glycerol derived from biodiesel production. Aspen Plus and Aspen ICARUS were used for the simulation and economic evaluation, respectively [20]. Espinosa et al. simulated the production process of biobutanol and hydrogen from palm oil production residues using UNISIM software. The simulation results served as the basis for the environmental assessment and energy integration of the process [21]. Niño-Villabos et al. conducted a techno-economic and environmental analysis of a biorefinery topology that produces biodiesel and hydrogen from oil extracted from African palm and Jatropha curcas. The information required for the analyses was gathered from a simulation performed in UNISIM [22]. Capdevila et al. simulated the production of bioethanol from rice husk fermentation using Aspen Hysys software, along with a parametric sensitivity analysis [23]. Herrera-Rodríguez et al. simulated the extraction of avocado oil from the pulp as an alternative for valorizing non-commercialized avocados. The Aspen Plus simulator was used to model the process, and the validation of the properties yielded positive results (accuracy greater than 90%) [24].

Although there is literature on the simulation of bioprocesses, very few studies address production at an industrial scale (high processing capacity). Therefore, the aim of this work is to simulate the industrial-scale production process of chitosan from shrimp exoskeletons. For this purpose, the commercial simulator Aspen Plus was used, fed with data from the literature and experimental results obtained by the authors. Additionally, the various operating parameters considered are detailed, along with a validation of the simulation through compa-

rison between the chitosan properties generated by the simulator and those reported in the literature. Moreover, the process efficiency in terms of yield is analyzed using technical performance indicators. This work is expected to contribute relevant information for the implementation of bioprocesses within the framework of a circular economy. Finally, this simulation is intended to serve as a basis for further analyses or evaluations under sustainability criteria.

METHODOLOGY

Figure 1 illustrates the methodology followed for the development and evaluation of a process to utilize shrimp exoskeletons for chitosan production. Initially, data related to the process are gathered from sources such as scientific literature, laboratory experiments, or pilot plant trials. Based on this information, the raw material, processing operations, and their operating conditions, among other aspects, are defined. From the collected data, a block diagram is designed to establish a preliminary process scheme and to perform a mass balance that identifies all mass flows and their respective compositions within the process.

Based on the diagram and the preliminary mass balance, the process simulation is built using Aspen Plus v12. This software was chosen due to its sequential modular approach, which enables robust modeling of conceptual processes at various scales (e.g., industrial scale), with support for a wide range of operations, chemical substances, and more [24]. The simulation begins with the selection of substances or compounds stored in the software's database. If a substance is not available, it is added using characterization data from the literature. Subsequently, the appropriate thermodynamic model is selected, considering the nature of the substances, operating conditions, and types of operations to be performed. From there, suitable unit operation models are selec-

ted from the available options in the software. Each of these models is then provided with the necessary input data (equipment parameters, mass flows, temperature, pressure, reactions) to carry out the internal calculations. Once the simulation is completed, the results are verified through a direct comparison of specific variables or parameters with bibliographic references or substance specification sheets. Finally, an evaluation of technical performance parameters is carried out to determine the efficiency of the process and to identify potential opportunities for process improvement.

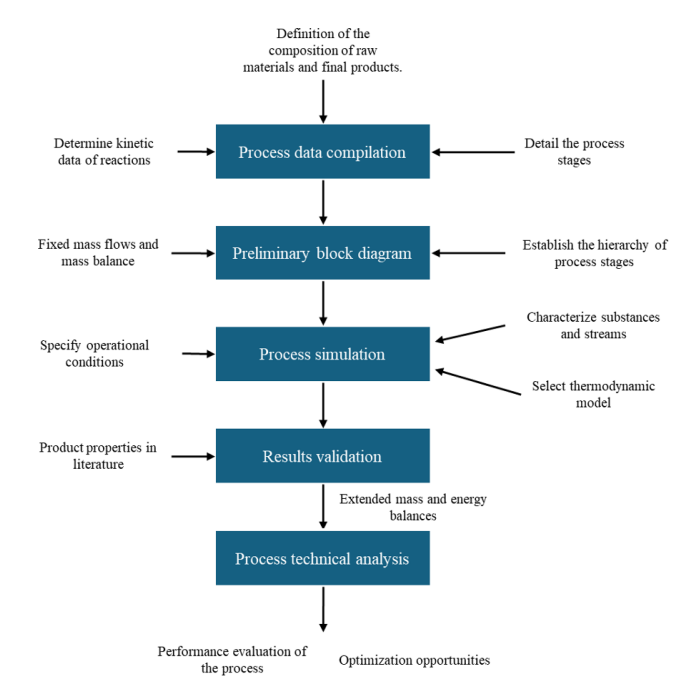


Fig. 1. Schematic representation of the methodology used.

Description of the chitosan production process from shrimp exoskeleton

Figure 2 shows the process diagram for chitosan production from shrimp waste. The production capacity (57,000 tons/year) was established by assuming a 10% availability of the total shrimp production capacity in Colombia (and other countries near the Pacific). This baseline corresponds to a 50% yield of the maximum amount of this waste [25]. The pro-

cess was carried out using stoichiometric reactions for each main stage, including demineralization, deproteinization, and deacetylation reactions [26]. The proposed large-scale chitosan production process consists of five main stages: (i) pretreatment, (ii) demineralization, (iii) neutralization, (iv) deproteinization, and (v) deacetylation. The shrimp exoskeleton is initially subjected to a pretreatment stage that includes washing, drying, and grinding to remove impurities and reduce particle size to a powder of 0.5 mm. Next, the treated exoskeleton is sent to the decolorization unit, where astaxanthin is extracted using a stream of 85% ethanol (solvent) [27].

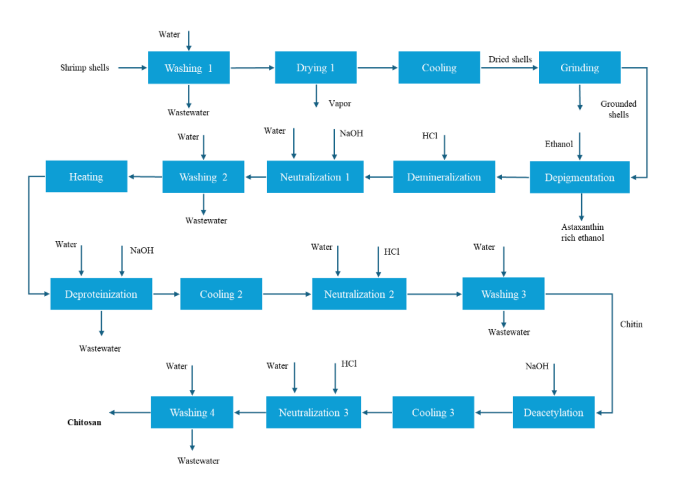


Fig. 2. Block diagram of chitosan production from shrimp exoskeleton.

Immediately, the resulting stream is sent to the demineralization unit, where minerals (CaCO₃, Na₂CO₃, MgCO₃) are removed through a series of reactions by adding a 1.5 M hydrochloric acid (HCl) solution, which prevents chitin hydrolysis [28]. After the demineralization reaction, the main stream is neutralized (neutralization reaction) with sodium hydroxide (NaOH) and washed to maintain a neutral pH [29]. Next, the proteins present in the shrimp exoskeleton are removed in the deproteinization unit (chemical reactions) by adding a NaOH solution, resulting in chitin as the final product [25]. The chitin extracted from this stage enters another neutralization stage, which uses an HCl stream along with a wash to adjust the pH to 7 [30]. Subsequently, the chitin enters the deacetylation sta-

ge, where the acetyl groups present in it are removed to convert it into chitosan. The chemical reaction in this stage is highly endothermic (requires high temperatures) and necessitates a large concentration of sodium hydroxide [31], [32]. This synthesis was previously developed under laboratory conditions by the authors. Next, the obtained chitosan is sent to neutralization stages with HCl and washed to adjust its pH [30]. Finally, the residual washing water must be removed from the produced chitosan.

Simulation of the chitosan production process from shrimp waste.

Component selection and raw material specification

In Table 1, the chemical composition of the shrimp exoskeleton used as raw material is presented. The main components include water, L-glutamic acid, lysine, D-N-acetylglucosamine, and astaxanthin. This composition is based on laboratory analyses conducted by the authors and studies found in the literature.

TABLE I
RAW MATERIAL COMPOSITION

Compound	Composition (% weight)
Methyl palmitate	0,2947
Astaxanthin	0,0023
CaCO ₃	0,0288
$\operatorname{Ca_3(PO_4)_2}$	0,0723
Na_2CO_3	0,0147
$MgCO_3$	0,0085
L-alanine,-N-L-alanyl	0,0362
D-N-acetylglucosamine	0,1682
L-glutamic-acid	0,0624
L-phenylalanine	0,0235
Methionine	0,0211
Lysine	0,0682
Water	0,2053

In Table 2, the compounds selected for the simulation of the industrial-scale chitosan production process are shown. To begin the simulation,

various compounds found in shrimp shells, such as astaxanthin to lysine, were chosen. All the compounds constituting the raw material are available in the substance databases of the simulator. Additionally, substances required for processing shrimp shells, such as water, solvents, secondary reagents, etc., were included. Each compound in the process was categorized based on its characteristics as either "conventional" or "solid." This classification is essential as it helps in selecting the appropriate method for modeling their properties with greater accuracy, ensuring that the simulation is as precise as possible.

TABLE II

COMPOUNDS USED FOR THE SIMULATION OF THE CHITOSAN PRODUCTION PROCESS FROM SHRIMP.

Compound	Туре	Formula
Methyl-palmitate	Conventional	C ₁₇ H ₃₄ O ₂ -N ₁
Astaxanthin	Solid	$C_{40}^{}H_{52}^{}O_{4}^{}$
Calcium-carbonate-calcite	Solid	CaCO ₃
Calcium-phosphate	Solid	$Ca_3(PO_4)_2$
Sodium-carbonate	Solid	Na ₂ CO ₃
Magnesium-carbonate	Solid	$MgCO_3$
L-alanine,-N-L-alanyl-	Solid	$C_6H_{12}N2O_3-N_2$
Carbon-dioxide	Conventional	CO_2
Magnesium-chloride	Conventional	$\mathrm{MgCl}_{\scriptscriptstyle 2}$
Calcium-chloride	Conventional	$CaCl_2$
Hydrogen-chloride	Conventional	HCl
D-N-acetylglucosamine	Solid	$C_8H_{15}NO_6$
L-glutamic-acid	Solid	$C_5H_9NO_4$
L-phenylalanine	Solid	$C_9H_{11}NO_2$
Orthophosphoric-acid	Conventional	H_3PO_4
Methionine	Solid	$C_5H_{11}NO_2S$
Lysine	Solid	$C_6^{}H_{14}^{}N_2^{}O_2^{}$
Water	Conventional	H_2O
Ethanol	Conventional	C_2H_6O
Sodium-hydroxide	Conventional	NaOH
Sodium-chloride	Conventional	NaCl
Chitosan	Solid	$C_6H_{13}NO_5$
Sodium-acetate	Conventional	$C_2H_3NaO_2$

Detailed specification of the simulation flowsheet for the chitosan production process

For the simulation of the chitosan production process from shrimp exoskeleton, the following considerations were defined: The methodology adopted for the development of the simulation includes the sequential development of convergence by section, considering a steady-state and without loss factors associated with the location.

The pretreatment stage consists of a washing unit, a drying unit, and a grinding unit. For the washing unit, the **SWash** model from the **solids** section of the model palette was used. This model requires defining a value for the solid-to-liquid (water) ratio along with a mixing efficiency, both of which were set to 1. For the drying stage of the exoskeleton, the *dryer* model was used in a *shortcut* configuration, where an operating temperature of 106°C (380K) was defined, and the moisture content was specified as 0. Before the size reduction stage, a cooling unit was placed, using the standard heat exchanger model *heater*, where a desired temperature of 25°C (298K) was established. For the grinding unit, the *crusher* model was used; this model requires defining the desired particle size, which in this case was set to 0.5 mm, and a mechanical efficiency of 1 was considered.

For the de-pigmentation unit, a component separation model (*sep*) was used, in which an 85% weight ethanol stream was employed as the solvent (separation agent). This model only requires defining the output composition based on the undesired components that need to be removed from the mainstream, in this case, for astaxanthin, it was set to 1. In the same way, both the water in the stream and the ethanol are completely separated from the processed stream.

For the demineralization stage, the *rstoic* model was used, which simulates the mineral removal reactions from the raw material. The model operates based on calculations derived from mass and energy balances from a macroscopic viewpoint, using data such as conversion,

stoichiometric reaction relationships, among others [33]. For the reactor, the stoichiometric equations for the demineralization of shrimp exoskeleton were established (1)-(4). In these reactions, inorganic minerals like calcium carbonate () react with hydrochloric acid to form removable salts, water, and carbon dioxide.

$$CaCO_3 + 2 HCl \rightarrow CaCl_2 + H_2O + CO_2$$
(1)

$$Na_2CO_3 + 2 HCl \rightarrow 2 NaCl + H_2O + CO_2$$
 (2)

$$MgCO_3 + 2HCl \rightarrow MgCl_2 + H_2O + CO_2$$
(3)

$$Ca_3(PO_4)_2 + 6 HCl \rightarrow 3 CaCl_2 + 2 H_3 PO_4$$
 (4)

For this model, a temperature of 25° C and a pressure of 1 bar were set. Additionally, a conversion of 1 was defined, and the reaction heats were calculated using a method based on reference values within the software. Furthermore, a stream of hydrochloric acid diluted to 5% by weight in water was defined under the same conditions (pressure and temperature) as the reactor.

For the deproteinization unit, the separation model *sep* was used, where the deproteinization reactions (5)-(9) take place. However, for the simplification of the simulation, these operations were treated as a standard separation based on the fractionations obtained from previous laboratory-scale studies. This was done by specifying the composition of the output stream, considering a separation degree of 1 for all undesirable proteins.

$$CaCO_3 + 2 HCl \rightarrow CaCl_2 + H_2O + CO_2$$
 (1)

$$Na_2CO_3 + 2 HCl \rightarrow 2 NaCl + H_2O + CO_2$$
 (2)

$$MgCO_3 + 2HCl \rightarrow MgCl_2 + H_2O + CO_2$$
(3)

$$Ca_3(PO_4)_2 + 6 HCl \rightarrow 3 CaCl_2 + 2 H_3 PO_4$$
 (4)

The operating conditions of the unit were established under the same pressure and temperature conditions as the previous units (25°C and 1 bar). Additionally, a stream of sodium hydroxide diluted to 2% by weight in water was introduced.

For the deacetylation unit, the *rstoic* model was employed, just like in the demineralization unit. Stoichiometric reactions were used for the deacetylation reaction (10), in which chitin is converted into chitosan by reacting with a stream of sodium hydroxide.

$$C_8H_{15}NO_6 + NaOH \rightarrow C_6H_{13}NO_5 + C_2H_3NaO_2$$
 (10)

The operating conditions of the unit were established under the same pressure and temperature conditions as the previous units (25°C and 1 bar). Additionally, a conversion of 1 was defined, and the reaction heats were calculated using a method with reference values within the software. Furthermore, a stream of sodium hydroxide diluted to 2% by weight in water was specified.

The neutralization stages are modeled in the same way as the demineralization unit, using a *rstoic* model. In this model, a stoichiometric reaction (11) is used to convert the residual hydrochloric acid or sodium hydroxide into conventional sodium chloride salts.

For the model, operating conditions similar to those used in the demineralization reaction model were applied: a temperature of 25 °C and a pressure of 1 bar. The conversion was set to 1. Additionally, the heat of reaction was calculated using reference data from the software under standard conditions (25 °C and 1 bar). Moreover, a stream of sodium hydroxide diluted to 2% in water was defined.

$$HCl + NaOH \rightarrow NaCl + H_2O$$
 (11)

Table 3 compiles the considerations made for each of the stages and units that make up the studied

process. Additionally, the relevant parameters for the convergence of each of the models are specified along with their respective values, including the origin, whether estimated, calculated, or the reference from where each one is extracted.

 $TABLE\ III$ Summary of the relevant parameters of the industrial-scale chitosan production process.

Stage	Unit	Parameter	Value	Reference
	Washing	Liquid-solid ratio	1	Assumed
Pretreat-		Mixing efficiency	1	Assumed
ment stage	Drying	Output wet	0	Assumed
8-		Temperature	106°C	[34]
	Cooling	Temperature	25°C	[34]
	Grinding	Output size	0.50 mm	
		Solvent mass flow (ethanol)	27,714 kg/h	Calculated
Depig- menta- tion stage	Asta- xanthin removal	Solvent mass fraction (%wei- ght/weight)	85%	[35]
		Separation efficiency	1	Assumed
Demine- ralization		Temperature	25°C	[34]
		Pressure	1 bar	[34]
	Demine- ralization reactor	Reaction		[36]
stage		Conversion	1	
		Hydrochloric acid mass flow	$62{,}326\mathrm{kg/h}$	Calculated
		Concentration (%weight/weight)	5%	[27]
		Reaction		[34]
Neutra- lization stage 1	Neutra- lization reactor	Conversion	1	
	Washing 2	Water mass flow	$23{,}051\mathrm{kg/h}$	Calculated
		Minerals separa- tion efficiency	1	Assumed
	Heating (exchan- ger)	Temperature	90°C	Assumed

Property model selection

		Sodium hydroxi- de mass flow	115,991 kg/h	Calculated
Deprotei- nization	Deprotei- nization	Concentration (%weight/weight)	2	[27]
stage	reactor	Reaction	$\begin{array}{l} C_6H_{12}N_2O_3 \\ + 2NaOH \\ \rightarrow 2C_3H_6NNaO_2 \\ + H_2O \\ C_{10}H_{16}N_2O_7 \\ + 2NaOH \\ \rightarrow 2C_5H_8NNaO_4 \\ + H_2O \\ C_{18}H_{20}N_2O_3 \\ + 2NaOH \\ \rightarrow 2C_9H_{10}NNaO_2 \\ + H_7O \\ C_{10}H_{20}N_2O_3S_2 \\ + 2NaOH \\ \rightarrow 2C_5H_8NNaO_4S_2 \\ + H_2O \\ C_{12}H_{26}N_4O_3 \\ + H_2O \\ C_{12}H_{26}N_4O_3 \\ + H_2O \\ C_{12}H_{26}N_4O_3 \\ + 2NaOH \\ \rightarrow 2C_6H_{13}N_2NaO_2 \\ + H_2O \\ C_{12}H_{26}N_4O_3 \\ + 2NaOH \\ \rightarrow 2C_6H_{13}N_2NaO_2 \\ + H_2O \\ \end{array}$	
		Conversion	1	Assumed
		Separation efficiency	1	Assumed
	Cooling	Temperature	25°C	[34]
		Temperature	25°C	[34]
	Neutra-	Reaction	$\begin{array}{l} HCl + NaOH \\ \rightarrow NaCl + H_2O \end{array}$	
	lization reactor 2	Conversion	1	Assumed
Neutra- lization stage 2	7646107 2	Hydrochloric acid flow	$4{,}282\mathrm{kg/h}$	Calculated
		Concentration (%weight/weight)	3	
		Water mass flow	$96{,}132\mathrm{kg/h}$	Calculated
	Washing 3	Washing water mass flow	57,679 kg/h	Calculated
	washing 5	Minerals separa- tion efficiency	1	
		Chitin lost in wastewater	17%	
	Cooling 2	Temperature	25°C	[34]
		Sodium hydroxi- de mass flow	99,075 kg/h	Calculated
Deace-	Deace- tylation	Concentration (%weight/weight)	2	[32]
	reactor	Reaction tempe- rature	110°C	[37]
tylation stage		Reaction		[26]
		Conversion	1	
	Cooling	Temperature	25°C	[34]

Neutraliza-	Neutra-	Temperature	25°C	[34]
	lization reactor 3	Reaction	HCl+NaO- H→Na- Cl+H ₂ O	
tion stage		Conversion	1	
		Hydrochloric acid mass flow	159,079 kg/h	Calculated
		Concentration (%weight/weight)	1	
		Water mass flow	$96{,}132\mathrm{kg/h}$	Calculated
	Was- hing 3	Washing water mass flow	89,353 kg/h	Calculated
		Minerals separation efficiency	1	

For the selection of property models, the aggregation state of the compounds, the type of unit operations, and the operating conditions (pressure and temperature) were considered as criteria. For the first criterion, a wide variety of compounds in solid state were found within the process streams. On the other hand, regarding the operating pressure and temperature conditions, most of the unit pressures are at ambient conditions with temperatures ranging from low to moderate. Considering the conditions described above, the SOLIDS method was selected using the software's method selection assistant. This chosen method allows for modeling a wide range of solid substances and their properties. It also models the different stages or unit operations of solid processing (such as crushing and sieving), such as the pre-treatment stage of solids like shrimp shells [38]. At the same time, the method allows modeling reactions with a solid phase between solid-fluid compounds, as done in the deacetylation stage. For gases and liquids within the process, the previous method uses *IDEAL* models. For the gaseous phase, the ideal gas law equation (eq.12) is used, where P is pressure; v, volume; n, moles of the gas; R, the ideal gas constant; and T, temperature.

In the case of the liquid phase, the model con-

$$Pv = nRT \tag{12}$$

forms to Raoult's law and Henry's law, where the activity coefficient is equal to 1 (γ = 1). This model is effective for pressure conditions below two bars (1.97 atm) and for both low and/or high temperatures. Additionally, it is important to highlight that the choice is based on the operational conditions of the process with an emphasis on the handling and processing of solids.

Technical analysis of the chitosan production process at an industrial scale

From the simulation, relevant information about the process is collected, which serves to evaluate the process performance in terms of efficiency for chitosan production. This analysis involves the quantification of indicators related to the process flows, such as raw material, water flow, and product flow, among others. Table 4 shows different performance indicators based on previous works by the authors [12], [40]. The considered indicators focus on raw material handling and the efficiency of transforming it into the desired product (chitosan) without considering by-products.

 $\begin{tabular}{l} Table IV \\ Technical performance indicators for the studied \\ Process. \end{tabular}$

Variable	Unit	Description	Equation
Production yield (Y)	g/kg	Product mass in grams per raw material mass per hour	$rac{\dot{m_P}}{\dot{m_{RM}}}$
Technical efficiency (Et)	(%)	Product mass per hour relative to the maximum possible produc- tion per hour	$rac{\dot{m_P}}{m_{P,m\acute{a}x}} otag 100\%$

RESULTS AND ANALYSIS

Figure 2 shows the flow diagram of the industrial-scale chitosan production process simulation from shrimp exoskeleton in Aspen Plus ® simulator. The simulation was divided into 8 stages:

a pretreatment unit, a pigment removal unit, a demineralization unit, a deproteinization unit, and 3 neutralization units. In the simulation, stream 1 entered the washing unit (WASHING1) of the pretreatment stage to be washed with stream 2, which is water. This stream 1 consists of shrimp exoskeleton as the raw material, with the composition of this stream defined in Table 1, under standard conditions (25°C and 1 bar) and a flow rate of 6,602.4 kg/h. The water stream has the same conditions but with a flow rate of 65,024 kg/h. The resulting streams from this unit are stream 3 and stream 4. Stream 3 is wastewater that carries the palmitate from the raw material, which is separated by more than 90%, approximately. Stream 4 is the main shrimp exoskeleton stream, free from methyl palmitate, but with significant moisture (approximately 90% by weight). This mainstream (stream 4) immediately entered the drying unit (DRYING) where all the water was removed from the stream, which was immediately separated as vapor at a temperature of 107°C in stream 5. Then, the dried raw material (stream 6) was cooled to 25°C before entering the milling process, which was done using a heat exchange device (COO-LING1). The cold stream (stream 7) entered the crusher (CRUSHING), where the raw material size was reduced to 0.5 millimeters.

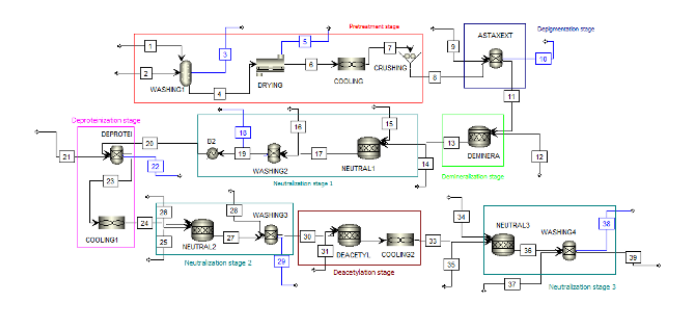


Fig. 3. Simulation flowsheet of the ndustrial-scale chitosan production process from shrimp exoskeleton.

The crushed exoskeleton (stream 8) exited the pretreatment stage and entered the pigment remo-

val stage (ASTAXENT) of the exoskeleton (astaxanthin) using a stream (stream 9) of 85% ethanol by weight, with a flow of 27,714 kg/h. The astaxanthin was removed from the crushed exoskeleton by contact with ethanol (affinity) with 100% efficiency. In this same unit, the astaxanthin-rich stream exited in stream 10, containing a small fraction of D-N-acetylglucosamine (5%), and most of the water and ethanol used. The pigment-free stream (stream 11) then passed to the demineralization reactor (DES-MINERA), where the inorganic minerals from the exoskeleton matrix were removed using 62,326 kg/h of 5% hydrochloric acid solution (stream 12). These reactions were carried out under standard pressure and temperature conditions (25°C and 1 bar), with 100% conversion. Immediately after, the resulting stream (stream 17) entered the first neutralization stage (NEUTRAL1), where the pH of the stream was maintained by neutralizing bases or acids. In this case, the hydrochloric acid in the stream was treated with a 2% sodium hydroxide solution by weight with a mass flow rate of 114,077 kg/h (stream 14), forming conventional salts (sodium chloride).

The treated stream (stream 17) immediately enters a washing zone (WASHING2) where all these salts are removed with 23,051 kg/h of water (stream 16) and are completely removed from the mainstream in a wastewater stream (stream 18). The washed stream (stream 19) passes through a heat exchanger (B2) where it is heated to a temperature of 90°C in preparation for entering the deproteinization unit. In the deproteinization unit (DEPRO-TEI), chitin is purified from the other proteins present in the shrimp exoskeleton. This purification is carried out using a 2% w/w sodium hydroxide solution with a flow of 115,999 kg/h (stream 21). The deproteinization reactions have a 100% conversion. In this same unit, a residual sodium hydroxide flow exits (stream 22).

Next, the stream containing chitin (stream 23) is cooled (COOLING1) to 25°C and is sent (stream 24) to the second neutralization stage (NEUTRAL2).

In this stage, the chitin stream comes into contact with a 43,282 kg/h stream of 3% w/w hydrochloric acid (stream 25) to remove any remaining NaOH and is immediately washed (WASHING3) with a 96,132 kg/h stream of water (stream 28). The residual stream (stream 29) from the washing stage contains proteins and unreacted compound residues. The treated chitin stream (stream 30) enters the deacetylation stage (DESACETIL) where chitosan is produced via deacetylation reactions with 100% conversion. The reaction takes place at 110°C and 1 bar pressure. The chitosan stream is cooled in a cooling unit (COOLING2) to 25°C and sent to the final neutralization unit with 2% w/w hydrochloric acid (NEUTRAL3). The remaining agents (NaOH and HCl) exit the system in a residual stream (stream 39) that is produced during the washing process (WAS-HING4).

Table 5 presents the operating conditions of the main streams in the industrial-scale chitosan production process. This table is derived from the extended mass balance along with the operational parameters specified within the software in the methodology section. The streams shown in the table are those that exit each stage of the simulation, except for stream 1, which is the feed (shrimp exoskeleton) to the process with a mass flow rate of 6,602 kg/h. Furthermore, most of the streams maintain a pressure and temperature similar to the feed (1 bar and 25°C), except for stream 20, which has a temperature of 90°C necessary to purify the chitin in the deproteinization stage. Stream 33 shows a mass flow rate of 110,789 kg/h, a value that, compared to the other streams in the table, indicates a high use of water as a medium for the process operations. Lastly, stream 39 is the product of the process, chitosan, with a flow rate of 1,387 kg/h, and it has a final water content of zero.

 $\label{thm:conditions} Table\ v$ Operating conditions of the main process streams.

Variable	1	8	11	13	20	24	30	33	39
	1	8	11	13	20	24	30	33	39
Temperature (°C)	25	25	25	25	90	25	25	25	25
Pressure (bar)	1	1	1	1	1	1	1	1	1
Mass flow (kg/h)	6,602	6,502	6,365	68,691	4,733	2,507	1,715	100,789	1,387
			Ma	iss compo	sition				
$C_{17}H_{34}O_2-N_1$	0.01	0	0	0	0	0	0	0	0
$C_{40}H_{52}O_4$	0	0.005	0	0	0	0	0	0	0
CaCO ₃	0.06	0.058	0.06	0	0	0	0	0	0
$Ca_3(PO_4)_2$	0.14	0.145	0.15	0	0	0	0	0	0
Na ₂ CO ₃	0.03	0.029	0.03	0	0	0	0	0	0
$MgCO_3$	0.02	0.017	0.02	0	0	0	0	0	0
${}^{\mathrm{C_6H}\text{-}}_{_{12}\mathrm{N2O_3}\text{-}\mathrm{N_2}}$	0.07	0.072	0.07	0.007	0.10	0	0	0	0
CO_2	0	0	0	0.004	0	0	0	0	0
$\mathrm{MgCl}_{\scriptscriptstyle 2}$	0	0	0	0.002	0	0	0	0	0
CaCl ₂	0	0	0	0.021	0	0	0	0	0
HCl	0	0	0	0.028	0	0	0	0	0
$\mathrm{C_8H_{15}NO_6}$	0.33	0.34	0.33	0.03	0.44	0.82	1	0	0
$C_5H_9NO_4$	0.12	0.12	0.13	0.01	0.17	0	0	0	0
$C_9H_{11}NO_2$	0.05	0.05	0.05	0	0.06	0	0	0	0
H_3PO_4	0	0	0	0.01	0	0	0	0	0
$C_5H_{11}NO_2S$	0.04	0.04	0.04	0.004	0.06	0	0	0	0
$C_6^{}H_{14}^{}N_2^{}O_2^{}$	0.12	0.12	0.13	0.01	0.17	0	0	0	0
$H_{_2}O$	0.01	0	0	0.86	0	0	0	0.96	0
C_2H_6O	0	0	0	0	0	0	0	0	0
NaOH	0	0	0	0	0	0.18	0	0.016	0
NaCl	0	0	0	0.003	0	0	0	0	0
$C_6H_{13}NO_5$	0	0	0	0	0	0	0	0.014	1
$C_2H_3NaO_2$	0	0	0	0	0	0	0	0.006	0
Total	1	1	1	1	1	1	1	1	1

Simulation results validation

In this stage, the simulation results are validated by the comparison of selected properties of the chitosan obtained from the flowsheet with data reported in the literature (experimental). Table 6 shows the accuracy achieved with the simulation of the chitosan production process from shrimp exoskeletons. The three properties collected from the literature were: the relative density of chitosan, molecular weight, and heat capacity.

TABLE VI							
COMPARISON OF CHITOSAN PROPERTIES AND THEIR ACCURACY.							
variable	variable unit literature simulatio acc						
			n				
relative density	$g*cm^{-3}$	1,38 ^A					
			1,58	86,7%			
molecular	g	179,09^	ŕ	,			
weight	* mol ⁻¹	,	179 17	99 95%			

132,79в

135

98,4%

 $g * Kg^{-1}$

* K⁻¹

А [39] В [40]

heat capacity

The results show that the selected properties exhibit high accuracy compared to the properties described in the literature for chitosan from shrimp waste. Both the molecular weight and heat capacity achieved an accuracy above 98%. However, the density showed a lower accuracy of 87%, which is due to the fact that the polymeric nature influencing this property was not rigorously accounted for (limitation of the software, especially for biopolymers). Nonetheless, these values indicate that the strategies employed in the simulation, the data packages, and the selected thermodynamic models are appropriate. It is worth noting that many of the studies reviewed report other properties for chitosan, such as the degree of deacetylation, degree of crystallinity, solubility, among others [41], which are usually analyzed for laboratory tests (experimental results). These properties could not be compared due to the limitations of the simulator, as in some cases several of these are already considered as technical parameters of certain models.

Technical analysis of the process production performance

Based on the equations provided in Table 4, the performance of the process for chitosan production is established. The process achieved, based on the technical considerations made, a yield of 210.1 grams of chitosan per kilogram of shrimp exoskeleton. This value is quite significant due to the high quantity of processed raw material (around 7,000 kg/h). At the same time, this yield can only be main-

tained if the process operates at maximum capacity. In contrast, the technical efficiency of the process reached 63.4%, indicating that the process efficiently converts a significant fraction of the chitin present in the raw material. There are some streams where the loss of this compound and its precursor occurs throughout the process, but it is not significant (individually), as is the case with wastewater streams. Similarly, this efficiency shows that the process has potential for improvement, particularly through the recovery of lost fractions in process effluents and the use of more efficient and selective separation units.

CONCLUSIONS

The utilization of shrimp industrial waste has become an economic opportunity for countries like Colombia. Compounds such as chitosan have generated significant interest as an important substitute for fossil-based compounds. However, the process is still in the early stages of development and requires refinement to reach its full potential. The simulation was performed in the Aspen Plus software based on information from literature and experimental data. The simulation built showed that is feasible the valorization of shrimp waste at a large scale, as technologies are available to produce significant quantities of chitosan. It's possible to produce 12,152 t/year of chitosan from 57,000 t/year of exoskeleton. The validation of chitosan properties showed a minimum accuracy of 88% compared to data reported in the literature. The generated simulation could be more robust by adding parameters that include the polymeric nature (structure) of chitosan. The technical analysis revealed a significant yield of 210.1 g per kilogram of raw material, thanks to its high processing capacity. At the same time, it has a considerable technical efficiency of 63.4%. This value indicates that the process converts a high fraction of the chitin present in the raw material; however, the process has room for improvement, as there are fractions that are not transformed in operations prior to the chitosan synthesis.

REFERENCIAS

- P. Söderholm, "The green economy transition: the challenges of technological change for sustainability," Sustain. Earth, vol. 3, no. 1, 2020, doi: 10.1186/s42055-020-00029-y.
- [2] S. Spierling et al., "Bio-based plastics A review of environmental, social and economic impact assessments," J. Clean. Prod., vol. 185, pp. 476–491, 2018, doi: 10.1016/j. jclepro.2018.03.014.
- [3] M. Palmeros Parada, P. Osseweijer, and J. A. Posada Duque, "Sustainable biorefineries, an analysis of practices for incorporating sustainability in biorefinery design," Ind. Crops Prod., vol. 106, pp. 105–123, 2017, doi: 10.1016/j.indcrop.2016.08.052.
- [4] F. A. Vicente et al., "Crustacean waste biorefinery as a sustainable cost-effective business model," Chem. Eng. J., vol. 442, no. March, 2022, doi:10.1016/j.cej.2022.135937.
- [5] H. El Knidri, R. Belaabed, A. Addaou, A. Laajeb, and A. Lahsini, "Extraction, chemical modification and characterization of chitin and chitosan," Int. J. Biol. Macromol., vol. 120, pp. 1181–1189, 2018, doi: 10.1016/j.ijbiomac.2018.08.139.
- [6] H. Zhang, S. Yun, L. Song, Y. Zhang, and Y. Zhao, "The preparation and characterization of chitin and chitosan under large-scale submerged fermentation level using shrimp by-products as substrate," Int. J. Biol. Macromol., vol. 96, pp. 334–339, 2017, doi: 10.1016/j.ijbiomac.2016.12.017.
- [7] I. Leceta, P. Guerrero, S. Cabezudo, and K. De La Caba, "Environmental assessment of chitosan-based films," J. Clean. Prod., vol. 41, pp. 312–318, 2013, doi: 10.1016/j. jclepro.2012.09.049.
- [8] S. Kumari, P. Rath, A. Sri Hari Kumar, and T. N. Tiwari, "Extraction and characterization of chitin and chitosan from fishery waste by chemical method," Environ. Technol. Innov., vol. 3, pp. 77–85, 2015, doi: 10.1016/j.

eti.2015.01.002.

- [9] P. S. Bakshi, D. Selvakumar, K. Kadirvelu, and N. S. Kumar, "Chitosan as an environment friendly biomaterial a review on recent modifications and applications," Int. J. Biol. Macromol., vol. 150, pp. 1072–1083, 2020, doi: 10.1016/j.ijbiomac.2019.10.113.
- [10] P. Pal, A. Pal, K. Nakashima, and B. K. Yadav, "Applications of chitosan in environmental remediation: A review," Chemosphere, vol. 266, p. 128934, 2021, doi: 10.1016/j.chemosphere.2020.128934.
- [11] V. B. Agbor, N. Cicek, R. Sparling, A. Berlin, and D. B. Levin, "Biomass pretreatment: Fundamentals toward application," Biotechnol. Adv., vol. 29, no. 6, pp. 675–685, 2011, doi: 10.1016/j.biotechadv.2011.05.005.
- [12] S. Meramo, A. Gonzalez-Quiroga, and A. Gonzalez-Del-gado, "Technical, Environmental, and Process Safety Assessment of Acetone-Butanol-Ethanol Fermentation of Cassava Residues," Sustain., vol. 14, no. 23, 2022, doi: 10.3390/sul42316185.
- [13] S. I. Meramo-Hurtado, K. Moreno-Sader, and A. D. González Delgado, "Evaluación ambiental de la producción a larga escala de microperlas de quitosano modificadas con tiourea como alternativa de valorización de residuos en el sector camaronicultor," Prospectiva, vol. 18, no. 1, pp. 1–6, 2020, doi: 10.15665/rp.v18i1.2100.
- [14] X. Mao, N. Guo, J. Sun, and C. Xue, "Comprehensive utilization of shrimp waste based on biotechnological methods: A review," J. Clean. Prod., vol. 143, pp. 814–823, 2017, doi: 10.1016/j.jclepro.2016.12.042.
- [15] L. Jacquemin, P. Y. Pontalier, and C. Sablayrolles, "Life cycle assessment (LCA) applied to the process industry: A review," Int. J. Life Cycle Assess., vol. 17, no. 8, pp. 1028–1041, 2012, doi: 10.1007/s11367-012-0432-9.
- [16] Z. D. King, "Aspen simulation of furfural and hydroxymethylfurfural production from biomass," p. 63, 2014.

- [17] W. C. Silva, E. C. C. Araújo, C. E. Calmanovici, A. Bernardo, and M. Giulietti, "Environmental assessment of a standard distillery using aspen plus®: Simulation and renewability analysis," J. Clean. Prod., vol. 162, pp. 1442–1454, 2017, doi: 10.1016/j.jclepro.2017.06.106.
- [18] C. Lopes, L. T. Antelo, A. Franco-Uría, A. A. Alonso, and R. Pérez-Martín, "Chitin production from crustacean biomass: Sustainability assessment of chemical and enzymatic processes," J. Clean. Prod., vol. 172, pp. 4140– 4151, 2018, doi: 10.1016/j.jclepro.2017.01.082.
- [19] D. A. Trirahayu, "Process simulation of glycerol production from corn oil via transesterification," IOP Conf. Ser. Mater. Sci. Eng., vol. 830, no. 2, pp. 7–11, 2020, doi: 10.1088/1757-899X/830/2/022011.
- [20] J. A. Posada, J. C. Higuita, and C. A. Cardona, "Optimization on the Use of Crude Glycerol from the Biodiesel Production to Obtain Poly-3-Hydroxybutyrate," Proc. World Renew. Energy Congr. Sweden, 8–13 May, 2011, Linköping, Sweden, vol. 57, pp. 327–334, 2011, doi: 10.3384/ecp11057327.
- [21] C. Espinosa, B. Arrieta, A. D. Gonzalez-Delgado, K. Ojeda, and E. Sanchez, "Technical and environmental evaluation of an integrated biorefinery from Residual biomass of oil palm fruit to obtain biobutanol and biohydrogen," J. Eng. Appl. Sci., vol. 13, no. 2, pp. 533–540, 2018, doi: 10.3923/jeasci.2018.533.540.
- [22] A. Ninō-Villalobos, J. Puello-Yarce, Á. D. González-Delgado, K. A. Ojeda, and E. Sánchez-Tuirán, "Biodiesel and Hydrogen Production in a Combined Palm and Jatropha Biomass Biorefinery: Simulation, Techno-Economic, and Environmental Evaluation," ACS Omega, vol. 5, no. 13, pp. 7074–7084, 2020, doi: 10.1021/acsomega.9b03049.
- [23] V. Capdevila, V. Kafarov, C. Gely, and A. Pagano, "Simulation of the Fermentation Process To Obtain Bioethanol From Rice Residues," vol. 6, no. 2, pp. 11–21, 2015.
- [24] T. Herrera-Rodríguez, V. Parejo-Palacio, and Á. Gon-

- zález-Delgado, "Computer-Aided Simulation of Avocado Oil Production in North Colombia," Chem. Eng. Trans., vol. 92, no. May, pp. 415–420, 2022, doi: 10.3303/CET2292070.
- [25] K. Cogollo-Herrera, H. Bonfante-Álvarez, G. De Ávila-Montiel, A. H. Barros, and Á. D. González-Delgado, "Techno-economic sensitivity analysis of large scale chitosan production process from shrimp shell wastes," Chem. Eng. Trans., vol. 70, pp. 2179–2184, 2018, doi: 10.3303/CET1870364.
- [26] D. Gómez-Ríos, R. Barrera-Zapata, and R. Ríos-Estepa, "Comparison of process technologies for chitosan production from shrimp shell waste: A techno-economic approach using Aspen Plus®," Food Bioprod. Process., vol. 103, pp. 49–57, 2017, doi: 10.1016/j.fbp.2017.02.010.
- [27] H. Bonfante-Alvarez, G. De Avila-Montiel, A. Herrera-Barros, M. Torrenegra-Alarcón, and Á. D. González-Delgado, "Evaluation of five chitosan production routes with astaxanthin recovery from shrimp exoskeletons," Chem. Eng. Trans., vol. 70, pp. 1969–1974, 2018, doi: 10.3303/CET1870329.
- [28] H. Srinivasan, K. Velayutham, and R. Ravichandran, "Chitin and chitosan preparation from shrimp shells Penaeus monodon and its human ovarian cancer cell line, PA-1," Int. J. Biol. Macromol., vol. 107, pp. 662–667, 2018, doi: 10.1016/j.ijbiomac.2017.09.035.
- [29] K. Moreno-Sader, S. I. Meramo-Hurtado, and A. D. González-Delgado, "Environmental sustainability analysis of chitosan microbeads production for pharmaceutical applications via computer-aided simulation, WAR and TRACI assessments," Sustain. Chem. Pharm., vol. 15, no. December 2019, 2020, doi:10.1016/j.scp.2020.100212.
- [30] J. Monter-Miranda et al., "Extracción y caracterización de propiedades fisicoquímicas, morfológicas y estructurales de quitina y quitosano," Rev. Mex. Ing. Química, vol. 15, no. 3, pp. 749–761, 2016.
- [31] E. F. Abadir, N. F. A. Salam, and F. I. Barakat, "Study on

- Production and Kinetics of Chitosan from Shrimp Shell Waste using Factorial Design Experimental Technique," J. Adv. Chem. Sci., vol. 5, no. 1, pp. 615–617, 2019, doi: 10.30799/jacs.204.19050103.
- [32] S. Zahedi, J. Safaei Ghomi, and H. Shahbazi-Alavi, "Preparation of chitosan nanoparticles from shrimp shells and investigation of its catalytic effect in diastereoselective synthesis of dihydropyrroles," Ultrason. Sonochem., vol. 40, no. February 2017, pp. 260–264, 2018, doi: 10.1016/j.ultsonch.2017.07.023.
- [33] E. Aguilar-Vásquez, M. Ramos-Olmos, and Á. D. González-Delgado, "A Joint Computer-Aided Simulation and Water-Energy-Product (WEP) Approach for Technical Evaluation of PVC Production," Sustainability, vol. 15, no. 10, 2023, doi:10.3390/sul5108096.
- [34] K. A. Moreno-Sader, J. D. Martinez-Consuegra, and Á. D. González-Delgado, "Development of a biorefinery approach for shrimp processing in North-Colombia: Process simulation and sustainability assessment," Environ. Technol. Innov., vol. 22, p. 101461, 2021, doi: 10.1016/j.eti.2021.101461.
- [35] A. Zuorro, K. A. Moreno-Sader, and Á. D. González-Delgad, "Inherent safety analysis and sustainability evaluation of chitosan production from shrimp exoskeleton in Colombia," Water (Switzerland), vol. 13, no. 4, 2021, doi: 10.3390/w13040553.
- [36] S. Meramo-Hurtado, C. Alarcón-Suesca, and Á. D. González-Delgado, "Exergetic sensibility analysis and environmental evaluation of chitosan production from shrimp exoskeleton in Colombia," J. Clean. Prod., vol. 248, 2020, doi: 10.1016/j.jclepro.2019.119285.
- [37] K. A. Moreno-Sader, J. Martínez-Consuegra, and Á. D. González-Delgado, "An integrated biorefinery approach via material recycle/reuse networks for the extraction of value-added components from shrimp: Computer-aided simulation and environmental assessment," Food Bioprod. Process., vol. 127, pp. 443–453, 2021, doi: 10.1016/j.fbp.2021.04.003.

- [38] F. L. Muñoz et al., "Insights from an exergy analysis of a green chemistry chitosan biorefinery," Chem. Eng. Res. Des., vol. 194, pp. 666–677, 2023, doi: 10.1016/j. cherd.2023.04.038.
- [39] Á. D. González-Delgado, K. A. Moreno-Sader, and J. D. Martínez-Consuegra, "Sustainable Biorefining of shrimp: Developments from Computer Aided Process Engineering (In Spanish)." Corporación Universitaria Minuto de Dios UNIMINUTO, 2022, doi: 10.26620/uniminuto/978-958-763-558-4.
- [40] S. Meramo, Á. D. González-Delgado, S. Sukumara, W. S. Fajardo, and J. León-Pulido, "Sustainable design approach for modeling bioprocesses from laboratory toward commercialization: Optimizing chitosan production," Polymers (Basel)., vol. 14, no. 1, 2022, doi: 10.3390/polym14010025.
- [41] I. O. Saheed, W. Da Oh, and F. B. M. Suah, "Chitosan modifications for adsorption of pollutants A review," J. Hazard. Mater., vol. 408, no. December 2020, p. 124889, 2021, doi: 10.1016/j.jhazmat.2020.124889.J. U. Duncombe, "Infrared navigation—Part I: An assessment of feasibility (Periodical style)," *IEEE Trans. Electron Devices*, vol. ED-11, pp. 34–39, Jan. 1959.